UDK 620.1:67.017:549.514.6
Original scientific article/Izvirni znanstveni članek

ISSN 1580-2949
MTAEC9, 54(6)777(2020)

ADSORPTION STRUCTURE PROPERTIES STUDY OF Cl_2 ON A RUTILE TiO_2(110) SURFACE WITH FIRST-PRINCIPLES CALCULATIONS

ŠTUDIJ ADSORPCIJSKIH STRUKTURNIH LASTNOSTI Cl_2 NA POVRŠINI RUTILA TiO_2(110) Z IZVORNIMI IZRAČUNI

Fan Yang[1,2], Liangying Wen[1,2*], Qin Peng[1,2], Yan Zhao[1,2], Jian Xu[1,2], Meilong Hu[1,2], Shengfu Zhang[1,2], Zhongqing Yang[3]

[1]School of Materials Science and Engineering, Chongqing University, Chongqing 400044, China
[2]Chongqing Key Laboratory of Vanadium-Titanium Metallurgy and Advanced Materials, Chongqing University, Chongqing 400044, China
[3]School of Power Engineering, Chongqing University, Chongqing 400044, China

Prejem rokopisa – received: 2020-06-22; sprejem za objavo – accepted for publication: 2020-07-15

doi:10.17222/mit.2020.034

Based on the ab-initio calculation method of the density-functional theory (DFT), the adsorptions of Cl_2 on a stoichiometric surface and reduced surface with bridge-oxygen defects of rutile TiO_2 (110) were compared and analyzed. The adsorption behavior and reaction mechanism of Cl_2 directly adsorbed on the TiO_2 (110) surface were analyzed by calculating the adsorption structure, adsorption energy, charge density and density of states. The results showed that the TiO_2 (110) surface with bridge-oxygen defects could promote the dissociation of Cl_2. The two Cl atoms dissociated form Ti6c-Cl bonds and Ti5c-Cl bonds with the TiO_2 (110) surface, which had one bridge-oxygen defect and one row of bridge-oxygen defects, respectively. There was some electron enrichment around these bonds. The stabilities of the Ti6c-O3c bonds and Ti5c-O3c bonds decreased. It was confirmed that more bridge-oxygen defects lead to higher stabilities of the adsorption system for the same kind of structures.

Keywords: titanium dioxide, bridge-oxygen defects, reduced surface, structure properties

Avtorji so na osnovi računskih metod funkcionalne teorije gostote (DFT) analizirali in primerjali adsorpcijo molekul Cl_2 na stehiometrični površini in površini, zmanjšani zaradi mostičkov kisikovih napak rutila TiO_2 (110). Adsorpcijo in reakcijske mehanizme Cl_2 direktno adsorbiranega na TiO_2 (110) površini, so analizirali z izračuni adsorpcijske strukture, adsorpcijske energije, gostote naboja in gostote stanj. Rezultati analiz so pokazali, da TiO_2 (110) površina z mostički kisikovih napak lahko pospeši disociacijo (cepitev) Cl_2. Pri dveh disociiranih atomih Cl iz Ti6c-Cl vezi in Ti5c-Cl vezi s TiO_2 (110) površine, ki ima eno vrsto mostičkov kisikovih napak, je prišlo do določene obogatitve z elektroni okoli teh vezi. Avtorji ugotavljajo, da se je stabilnost Ti6c-O3c vezi in Ti5c-O3c vezi zmanjšala in več kot je bilo mostičkov kisikovih defektov, večja je bila stabilnost adsorpcijskega sistema za enako vrsto strukture.

Ključne besede: titanov dioksid, premostitve kisikovih defektov (napak), zmanjšana površina, strukturne lastnosti

1 INTRODUCTION

Titanium dioxide is an important raw material for the coating production. After the rapid development of the coating industry in recent years, the demand for titanium dioxide is gradually increasing.[1,2] At present, an important intermediate stage in the titanium-dioxide production is the $TiCl_4$ preparation with fluidized chlorination,[3] which is the mainstream technology of the $TiCl_4$ production in the world. During fluidized chlorination, a mixture of titanium raw materials rich in TiO_2 and petroleum coke is fluidized under the action of chlorine gas and the Ti-O bonds within TiO_2 are continuously dissociated. This inevitably causes a reduced TiO_2 surface with bridge-oxygen defects, which may become an important unit for the preparation of $TiCl_4$ with chlorination, affecting the chlorination process and efficiency. Therefore, it is of great theoretical and practical significance to elucidate the micro-mechanism and reaction behavior.

*Corresponding author's e-mail:
cquwen@cqu.edu.cn (Liangying Wen)

The first-principle calculations of the density-functional theory (DFT) are used to study the reaction mechanisms of materials at the microscopic level, such as structural parameters, electron transfer, bonding process and so on. It has become an effective method to study the surface adsorption behavior of TiO_2 from the atomic point of view.[4,5] Many scholars have used the density-functional theory (DFT) to study the micro-mechanism of atomic adsorption on the TiO_2 (110) surface. X. Wu et al.[6] studied the adsorption behavior of O_2 and CO molecules on the TiO_2 (110) surface. It was found that O_2 and CO molecules could adsorb on the TiO_2 (110) surface with oxygen defects. When a CO molecule is oxidized to a CO_2 molecule by reducing the surface, the O_2 molecule fills in the oxygen defect and produces a new stoichiometric TiO_2 (110) surface.

Z. Yang et al.[7] studied the adsorption behavior of CO molecules on the stoichiometric TiO_2 (110) surface. It was found that the adsorption structure of OC-Ti was more stable than that of CO-Ti in the adsorption reaction, indicating that the adsorption behavior of CO on the

TiO_2 (110) surface was oriented. D. C. Sorescu et al.[8] studied the adsorption behavior of CO and NO on the surface of TiO_2 (110). It was found that the binding energy of the adsorption system was related to the reduced density of the TiO_2 (110) surface. The binding energy of the CO adsorption on the surface with one row of bridge-oxygen defects is about 4 times larger than that of the stoichiometric surface. At present, the adsorption in the chlorination reaction of a Cl_2 molecule directly on the stoichiometric surface and reduced surface of rutile TiO_2 (110) is rarely reported. It is necessary to study the reaction behavior and adsorption mechanism of Cl_2 molecules adsorbed on the stoichiometric surface and reduced surface of rutile TiO_2(110).

In this work, we have investigated the adsorption behavior of Cl_2 on the stoichiometric and reduced surface of rutile TiO_2 (110) based on the first-principle ab-initio calculation method of the density-functional theory (DFT). The results provided an important insight into the interaction mechanism of Cl_2 on the stoichiometric and reduced surface of rutile TiO_2 (110).

2 CALCULATION METHOD AND PARAMETER SELECTION

Based on the density-functional theory, the periodic structure of titanium dioxide is calculated using the Castep module of the Material Studio software package.[9–18] As shown in **Figure 1**, it mainly includes a stoichiometric rutile TiO_2 (110) surface, a reduced rutile TiO_2 (110) surface with one bridge-oxygen defect (1O surface) and a reduced rutile TiO_2 (110) surface with one row of bridge-oxygen defects (2O surface). In order to take into account the coulomb interaction between core electrons and nuclei, the plane-wave ultra-soft pseudopotential is used to simulate the electron potential in a free-electron system.[19–22] To facilitate the study of the interaction between free electrons and ions, the valence electrons are approximately regarded as free electrons.[23] The PBE-GGA[24] approach is introduced for exchange-correlation energy calculations. The model is composed of a 2 × 2 cell structure with 9 layers of atoms, and the energy cutoff is 400eV. During the calculation, all the atoms in the upper 3 layers are relaxed while the other 6 layers are fixed. The thickness of the vacuum layer is set to 15 Å and the K-point grid in the Brillouin zone is divided into 2 × 1 × 1. The convergence-tolerance values for the energy, maximum force, maximum stress and maximum displacement are 1×10^{-5} eV/atom, 0.03 eV/Å, 0.05 GPa and 0.001 Å, respectively. The specific parameters are shown in **Table 1**.

Table 1: Set of calculation parameters for the rutile TiO_2 (110) surface

Parameter	TiO_2(110)	
K-point	2×1×1	
Energy cutoff / eV	400	
Number of layers	9	
Fixed number of atomic layers	6	
Vacuum-layer thickness / Å	15	
Lattice parameters	a / Å	5.934
	b / Å	13.132
	c / Å	24.130

The stability of the system can be judged on the basis of the adsorption energy, ΔE. Adsorption energy ΔE is expressed with Equation 1:

$$\Delta E = E_{TiO_2+X} - (E_{TiO_2} + E_X) \quad (1)$$

where E_{TiO2+X} represents the energy of X (X = Cl_2) adsorbed on the stoichiometric surface or reduced surface with bridge-oxygen defects of TiO_2 (110), E_{TiO2} represents the energy of the stoichiometric surface or reduced surface with bridge-oxygen defects of TiO_2 (110), and E_X represents the energy of X (X = Cl_2).

3 RESULTS AND DISCUSSION

3.1 Adsorption of Cl_2 on the stoichiometric rutile TiO_2 (110) surface

3.1.1 Adsorption-structure analysis

Figure 2 shows three kinds of adsorption structures formed by Cl_2 adsorbed on the stoichiometric surface of TiO_2 (110). During the adsorption process, the chemical bonds of the Cl_2 molecule do not break and Cl_2 enters the

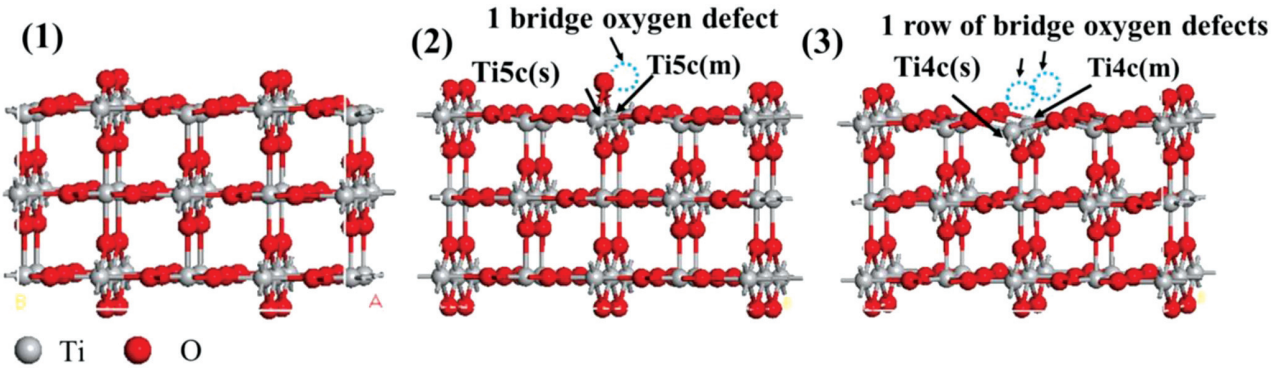

Figure 1: Side view of the calculated system: 1) stoichiometric surface of rutile TiO_2 (110); 2) reduced surface of rutile TiO_2 (110) with one bridge-oxygen defect (1O surface); 3) reduced surface of rutile TiO_2 (110) with one row of bridge-oxygen defects (2O surface)

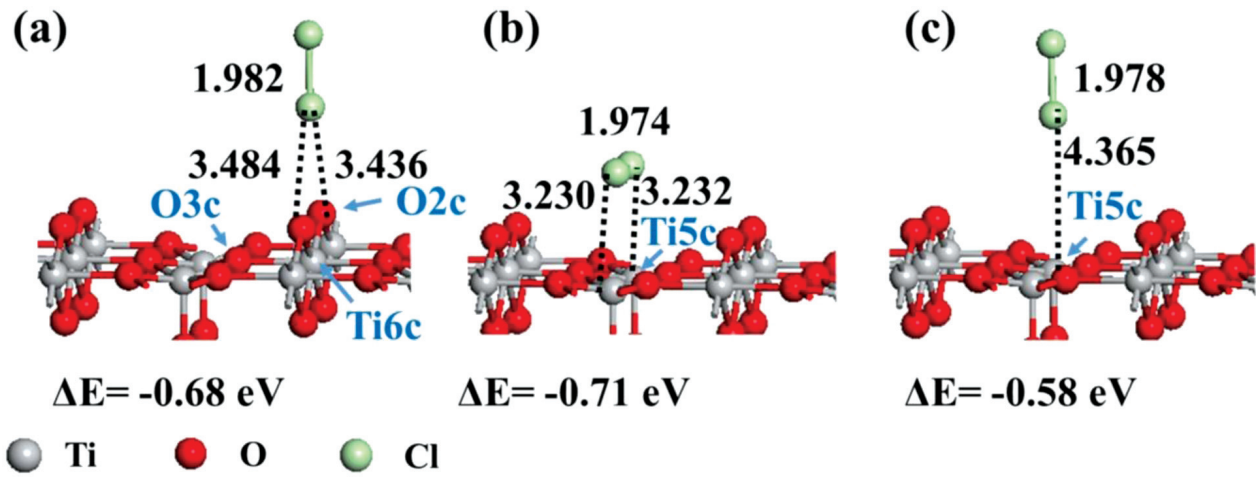

Figure 2: Adsorption structure of Cl_2 on the stoichiometric surface of rutile TiO_2(110): a) Cl_2 is perpendicular to the adsorption surface and above the oxygen atoms; b) Cl_2 is parallel to the adsorption surface; c) Cl_2 is perpendicular to the adsorption surface and above the titanium atoms

vacuum layer after the adsorption, indicating that there are no chemical bonds between Cl_2 and the stoichiometric surface of TiO_2 (110). Before the adsorption, the chemical-bond length of Cl_2 is 1.980 Å and after the adsorption, the chemical-bond lengths of Cl_2 in configurations (a), (b) and (c) in **Figure 2** are 1.982 Å, 1.974 Å and 1.978 Å, respectively. Among them, the bond length of Cl_2 from **Figure 2b** has changed significantly, with a decrease of 0.006 Å. In **Figure 2a**, the average distance between Cl_2 and surface O2c is 3.460 Å. In **Figure 2(b)**, the average distance between Cl_2 and surface Ti5c is 3.231 Å, and in **Figure 2c**, the distance between Cl_2 and surface Ti5c is 4.365 Å. Among them, the smallest distance between Cl_2 and the stoichiometric surface of TiO_2 (110) is in **Figure 2b**. The adsorption energies of configurations (a), (b) and (c) in **Figure 2** are –0.68eV, –0.71eV and –0.58eV, respectively. In the process of adsorption, the chemical bonds between the adsorbed molecules and TiO_2 (110) surface can be used to determine whether the process is a chemical adsorption or physical adsorption. It can be seen that the adsorption methods of these three systems are physical adsorption, and the interactions between Cl_2 and the stoichiometric surface of TiO_2 (110) are not obvious.

3.1.2 Charge analysis

Table 1 shows the Mulliken charge analysis of the Cl_2 adsorbed on the stoichiometric surface of TiO_2 (110). It can be seen that for the clean surface of TiO_2 (110) and the three structures including a), b) and(c) in **Figure 2**, all Ti6c(m) are electron providers, thus losing 1.26e, 1.26e, 1.28e and 1.27e, respectively. All O3c are electron recipients, obtaining 0.69e, 0.69e, 0.68e and 0.69e, respectively. In the structure from **Figure 2a**, Cl_2 obtains 0.01e from the surface of TiO_2(110) and in **Figure 2(b)**, Cl_2 transfers 0.08e to the surface of TiO_2(110), in which two Cl atoms lose 0.04e. In **Figure 2c**, there is no electron transfer between Cl_2 and the surface of TiO_2 (110). Ti6c, O3c and Cl_2 from the structure shown in **Figure 2b** lose electrons, namely 0.02e, 0.01e and 0.08e, respectively. Before the adsorption reaction, the Mulliken overlap population of the Cl-Cl bond in the Cl_2 molecule is 0.13e. After the adsorption reaction, the Mulliken overlap populations of Cl-Cl bonds in the (a), (b) and (c) structures are 0.13e, 0.19e and 0.13e, respectively. The results show that the adsorption reaction has little effect on the covalent bonding interactions of the Cl-Cl bonds in the Cl_2 molecules.

Table 2: Mulliken charge analysis of Cl_2 adsorption on the stoichiometric rutile TiO_2(110) surface

	Ti6c(m)		O3c		Cl_2	
	q(e)	Δq(e)	q(e)	Δq(e)	q(e)	Δq(e)
Cl_2	–	–	–	–	14.00	0.00
TiO_2 (110)	10.74	1.26	6.69	–0.69	–	–
(a)	10.74	1.26	6.69	–0.69	14.01	–0.01
(b)	10.72	1.28	6.68	–0.68	13.92	0.08
(c)	10.73	1.27	6.69	–0.69	14.00	0.00

*Δq(e) represents the electron gain or loss, a negative value represents an electron gain and a positive value represents an electron loss.

3.2 Adsorption of Cl_2 onto the rutile TiO_2(110) surface with bridge-oxygen defects

3.2.1 Adsorption-structure analysis

Figure 3 shows the adsorption structure of Cl_2 on the surface of TiO_2 (110) with bridge-oxygen defects. **Figures 3d** and **3e** show the adsorption structures of Cl_2 on the surface of TiO_2 (110) with one bridge-oxygen defect. In the structure from **Figure 3d**, the chemical bond of the Cl_2 molecule breaks and dissociates two Cl atoms. One Cl atom dissociates into the vacuum layer, while the other Cl atom occupies the surface bridge-oxygen defect and bonds with Ti5c (m) and Ti5c (s). At this time, Ti5c (m) and Ti5c (s) are transformed into Ti6c (m) and Ti6c (s), forming a Ti6c (m)-Cl bond and a Ti6c (s)-Cl bond with lengths of 2.385 Å and 2.431 Å, respectively.

The distance between the two Cl atoms extends to 3.213 Å. The length of the chemical bond between Ti6c (m) and Ti6c (s) extends from 2.721 Å to 2.819 Å. The length of the chemical bond between Ti6c (m) and O3c on both sides extends from 1.986 Å to 2.035 Å and 2.036 Å, respectively. In the structure from **Figure 3e**, the two Cl atoms dissociated from the Cl_2 molecule bond with Ti5c on both sides.. At this time, Ti5c is converted into Ti6c. The distance between the two Cl atoms extends to 3.113 Å, and the bond lengths of the two Ti6c-Cl are 2.570 Å and 2.575 Å, respectively. The coordination number of Ti5c on the original two sides increases and the activity decreases. The length of the chemical bond between T5c (m) and Ti5c (s) extends to 2.874 Å. The bond length of Ti5c (m)-O3c formed by Ti5c (m) and O3c on both sides increase by 0.072 Å and 0.073 Å after the adsorption reaction, respectively. The chemical-bond length between Ti5c (middle) and O2c extends to 1.754 Å, and Ti5c (m) and O3c are raised upward, indicating that the adsorption of Cl_2 has an effect on the relative position of surface atoms. The adsorption energies of the structures from **Figure 3d** and **3e** are –1.44 eV and –2.48 eV, respectively. The adsorption method of these two structures is chemical adsorption. It can be seen that **Figure 3e** exhibits a lower adsorption energy and higher stability.

Figures 3f and **3g** show the adsorption structures of Cl_2 on the surface of TiO_2 (110) with one row of bridge-oxygen defects. In the structure from **Figure 3f**, the chemical bond of the Cl_2 molecule breaks and dissociates two Cl atoms. One Cl atom dissociates into the vacuum layer, while the other Cl atom bonds with surface Ti4c (m). At this time, Ti4c is converted into Ti5c, forming a Ti5c (m)-Cl bond with a length of 2.221 Å, and the distance between the two Cl atoms extends to 2.721 Å. Ti5c (m) is obviously depressed downward, and the bond length of Ti5c (m)-O3c formed by Ti5c (m) and O3c on both sides are 1.981 Å and 1.982 Å, respectively. In the structure from **Figure 3g**, the two Cl atoms dissociated from the Cl_2 molecule bond with Ti4c (m) and Ti4c (s), respectively. At this time, Ti4c is converted into Ti5c, and the distance between the two Cl atoms extends to 2.973 Å, and the bond lengths of the two Ti5c-Cl are 2.230 Å and 2.231 Å, respectively. The coordination number of the original Ti4c increases and the stability improves. The bond lengths of Ti5c (m)-O3c bonds formed by Ti5c (m) and O3c on both sides are 1.994 Å. It is the same as before the adsorption. The adsorption energies of the structures from **Figures 3f** and **3g** are –1.60 eV and –4.24 eV, respectively. The adsorption method of these two adsorption structures is chemical adsorption. The adsorption energy of the structure from **Figure 3g** is lower and the stability is higher.

Among the above seven adsorption structures, the stability of adsorption structure increases with the increase of the number of bridge-oxygen defects on the surface. In **Figure 3**, the (d) structure with one bridge-oxygen defect is similar to the (f) structure with one row

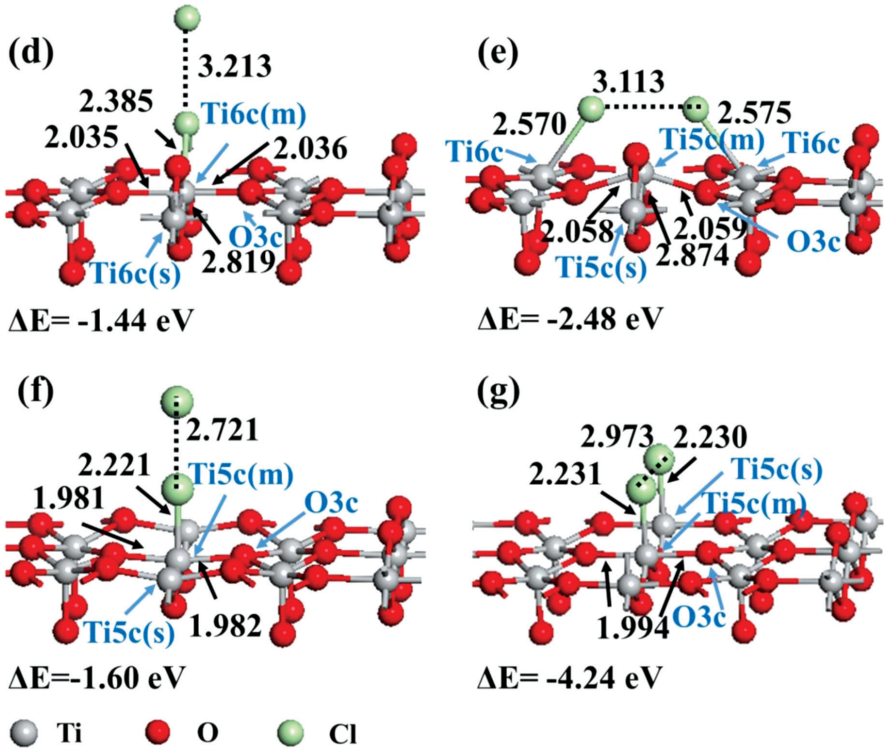

Figure 3: Adsorption structure of Cl_2 on the surface of rutile TiO_2(110) with bridge-oxygen defects; d) and e) the adsorption structures of Cl_2 on the surface with one oxygen defect (1O surface); f) and g) the adsorption structures of Cl_2 on the surface with one row of oxygen defects (2O surface)

of bridge-oxygen defects, and the adsorption energies are –1.44 eV and –1.60 eV, respectively. The stability of the (f) structure is higher than that of the (d) structure. The structure from **Figure 3(e)** with one bridge-oxygen defect is similar to the structure from **Figure 3(g)** with one row of bridge-oxygen defects, and the adsorption energies are –2.48 eV and –4.24 eV, respectively. The stability of the (g) structure is higher than that of the (e) structure. Configurations (a), (b) and (c) from **Figure 2** are without bridge-oxygen defects and the adsorption energies are relatively high, namely –0.68 eV, –0.71 eV and –0.58 eV, respectively, while their stabilities are relatively low. Therefore, for the same kind of structures, the stabilities of adsorption structures with one row of bridge-oxygen defects are higher, followed by the adsorption structures with one bridge-oxygen defect, and the stabilities of the adsorption structures without bridge-oxygen defects are lower. With the increase in the number of bridge-oxygen defects on the surface of TiO_2 (110), the Ti6c coordination number gradually decreases, and Ti6c is converted into Ti5c or Ti4c. It bonds more easily with the Cl atoms with stronger electronegativity, increasing the saturation and indicating that bridge-oxygen defects can promote the dissociation of Cl_2 and increase the probability of the Cl atoms bonding with Ti atoms on the surface. Moreover, the lower the saturation of Ti, the more Ti-Cl bonds are formed, and the stability of the adsorption structure is higher.

3.2.2 Charge analysis

Figure 4 shows the charge-density difference of the Cl_2 adsorbed on the surface of TiO_2(110) with bridge-oxygen defects, and the isosurface level is 0.05 electrons/Å^3. **Figures 4d** and **4e** show the charge-density difference of Cl_2 on a reduced surface with one bridge-oxygen defect. It can be seen from **Figure 4d** that the chemical bond of the Cl_2 molecule breaks and dissociates two Cl atoms. One Cl atom dissociates into the vacuum layer, while the other Cl atom occupies the bridge-oxygen defect on the surface to form a Ti6c-Cl bond. The area around the Ti6c-Cl bond is an electron-enriched region with a high electron density. In **Figure 4e**, both Cl atoms form Ti6c-Cl bonds. There are more electrons around the Ti6c-Cl bonds, belonging to the electron-enriched regions. These phenomena are similar to the ones from **Figures 4f** and **4g**. Cl atoms form Ti5c-Cl bonds and there are more electrons around the Ti5c-Cl bonds. There are more aggregated electrons around the Ti5c-Cl bond in **Figure 4g** than in **Figure 4e**, which shows that the covalent-bonding interaction of the Ti5c-Cl bond formed in the g) structure is stronger and its stability is relatively higher.

Table 2 shows the Mulliken charge analysis of Cl_2 adsorbed on the surface of TiO_2 (110) with bridge-oxygen defects. In the adsorption process, the Ti6c (m) in **Figure 3d** and the right Ti6c in **Figure 3e** are the electron providers on the surface of TiO_2 (110) with one bridge-oxygen defect, losing 1.26e, 1.18e and 1.26e, respectively. All O3c are the electron recipients, obtaining 0.72e, 0.70e and 0.64e, respectively. In **Figure 3d**, the Mulliken overlap population of the Ti6c(m)-Cl bond is 0.35e, and the Mulliken overlap populations of the Ti6c(m)-Cl bonds on both sides in **Figure 3e** are 0.33e and 0.34e, respectively. Among them, the Mulliken overlap population in the structure from **Figure 3d** is larger, indicating that the covalent bond between Ti6c(m) and Cl atom in the structure is stronger.

On the surface of TiO_2 (110) with one row of bridge-oxygen defects from **Figures 3f** and **3g**, all Ti5c (m) are the electron providers, losing 1.11e, 0.93e and 1.05e, respectively. All O3c are the electron recipients, obtaining 0.75e, 0.70e and 0.71e, respectively. The Mulliken overlap population of the Ti5c (m)-Cl bond in **Figure 3f** is 0.66e, and the Mulliken overlap populations of the Ti5c (m)-Cl bond and Ti5c (s)-Cl bond in **Figure 3g** are 0.82e. Among them, the Mulliken overlap populations of the Ti5c (m)-Cl bond and Ti5c (s)-Cl bond in the structure from **Figure 3g** are larger, indicating that the covalent-bonding interactions between Ti5c and Cl atoms on both sides of the structure are stronger. Comparing the adsorption of Cl_2 on the surface of TiO_2 (110) with one bridge-oxygen defect from **Figures 3d** and **3e**, the covalent bonding interactions of Cl_2 on the surface of

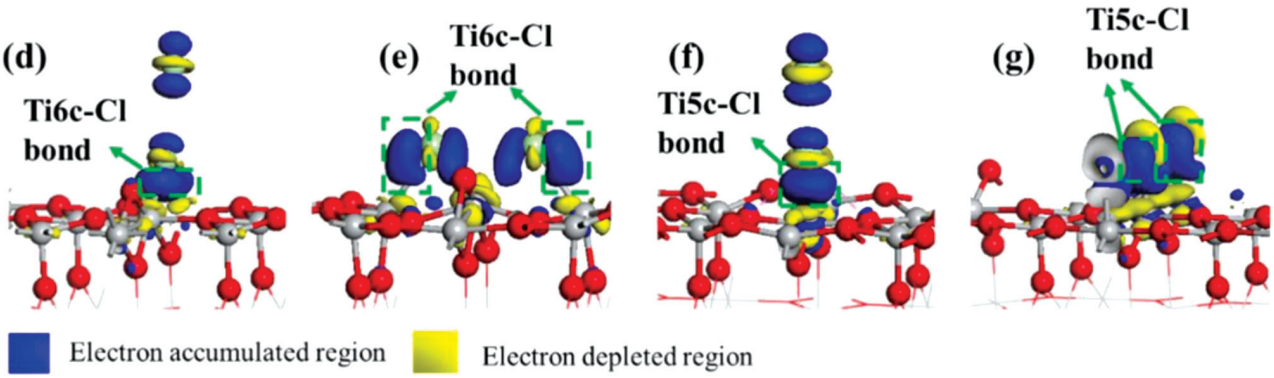

Figure 4: bonding charge density of Cl_2 adsorb on the surface with oxygen defects of rutile TiO_2 (110). The blue and yellow colors represent electron accumulated region and electron depleted region, respectively. Among them, d), e), f), g) are corresponding to d), e), f), g) from **Figure 3**

TiO_2 (110) with one row of bridge-oxygen defects are stronger.

Table 3: Mulliken-charge analysis of Cl_2 adsorbed on the surface with oxygen defects of rutile TiO_2 (110)

	Ti		O3c		Cl_2	
	q(e)	Δq(e)	q(e)	Δq(e)	q(e)	Δq(e)
1O surface	10.74	1.26	6.72	–0.72	–	–
(d)	10.82	1.18	6.70	–0.70	14.50	–0.50
(e)	10.74	1.26	6.64	–0.64	14.58	–0.58
2O surface	10.89	1.11	6.75	–0.75	–	–
(f)	11.07	0.93	6.70	–0.70	14.52	–0.52
(g)	10.95	1.05	6.71	–0.71	14.46	–0.46

*Δq(e) represents the electron gain or loss, a negative value represents an electron gain and a positive value represents an electron loss.

3.2.3 Density-of-state analysis

Figure 5 shows the partial density of states (PDOS) for Ti6c, Ti5c and O3c when Cl_2 is adsorbed on the TiO_2 (110) surface with bridge-oxygen defects. Among them, TiO_2-1O and TiO_2-2O are clean surfaces of TiO_2 (110) with one bridge-oxygen defect and one row of bridge-oxygen defects, respectively. **Figures 5d**and **5e** show the PDOSs of Cl_2 adsorbed on the surface of TiO_2 (110) with one bridge-oxygen defect. **Figures 5f** and **5g** show the PDOSs of Cl_2 adsorbed on the surface of TiO_2 (110) with one row of bridge-oxygen defects. Configurations (d), (e), (f) and (g) from **Figure 5** correspond to configurations d), e), f) and g) from **Figure 3**, respectively.

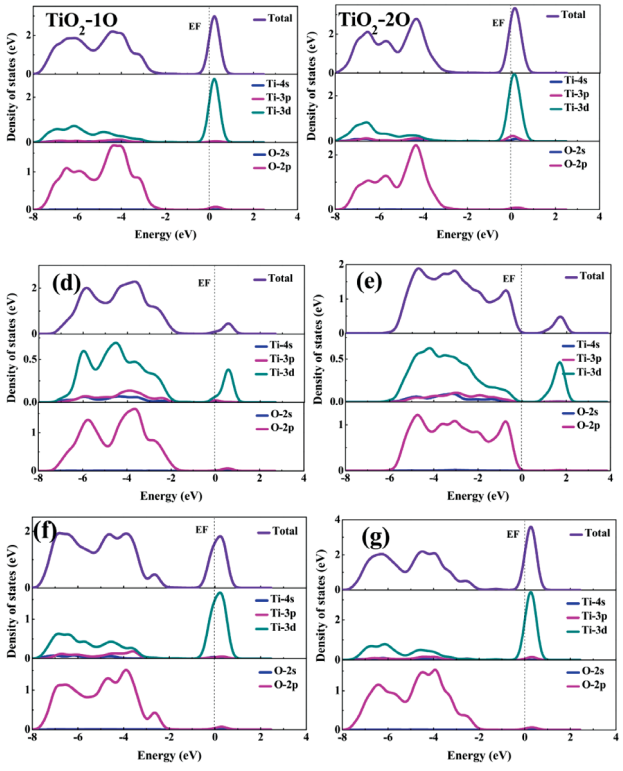

Figure 5: Partial density of states for the adsorption structure of Cl_2 on the 1O surface and 2O surface. Among them, TiO_2-1O and TiO_2-2O represent the TiO_2 (110) surface with one oxygen defect and one row of bridge-oxygen defects before the adsorption, respectively. Curves d), e), f), g) correspond to d), e), f), g) from **Figure 3**.

Figure 5 shows that the valence bands of the Ti6c-O3c bond and Ti5c-O3c bond on the surface of TiO_2 (110) before and after the adsorption are mainly contributed by the O2p orbital and the conduction band is mainly contributed by the Ti3d orbital. In **Figure 5** (TiO_2 (110)-1O), there are obvious resonance peaks at 0.208 eV on the right-hand side of the Fermi energy level for the Ti3d orbital and O2p orbital, indicating that there is a pd orbital hybridization between Ti6c and O3c, and there is an antibonding orbital between the two atoms. Compared with **Figure 5** (TiO_2 (110)-1O), on the left-hand side of the Fermi energy level, the valence-band density peaks of Ti6c and O3c obviously move to the Fermi energy level from **Figure 5d**, and there are resonance peaks at –3.642eV and –2.792eV in the Ti3d and O3p orbitals, respectively. This indicates that the bonding effect of Ti6c and O3c at a low level is weak and electrons transit more easily to the Fermi level. On the right-hand side of the Fermi-energy level, the PDOS peak of the Ti3d orbital shifts downward significantly, weakening the anti-bonding interactions between Ti6c and O3c. The stability of the Ti6c-O3c bond decreases and more electrons at a high energy level are transferred to the surrounding Cl atom, resulting in the formation of a new Ti6c-Cl bond. In **Figure 5e**, the PDOS peaks of theTi6c and O3c valence band move obviously to the Fermi energy level, and there are lower values of the resonance peaks of Ti6c and O3c at –4.758eV, indicating that the bonding between Ti6c and O3c is weakened. The PDOS peak of the density of states of O3c is concentrated in the higher-energy area on the left-hand side of the Fermi-energy level, indicating that the difficulty of electron transition to the higher-energy-level direction is reduced, and the delocalization is enhanced, while more electrons transfer around the Ti-Cl bond. On the right-hand side of the Fermi-energy level, the PDOS peak of Ti6c decreases obviously, the PDOS peaks of the Ti3d orbital and O2p orbital obviously move to the right-hand area, and the PDOS peak decreases, causing the resonance peaks of Ti6c and O3c in the anti-bonding orbital to be weakened, while the stability of the Ti6c-O3c bond decreases.

Figure 5 (TiO_2-2O) shows that there are resonance peaks at –6.584eV and –4.358eV for the Ti4d orbital and O2p orbital on the left-hand side of the Fermi energy level, respectively, indicating that there is an obvious bonding interaction between Ti5c and O3c. On the right-hand side of the Fermi-energy level, there are obvious resonance peaks for the Ti3d orbital and O2p orbital at 0.171eV. Comparing the curves from **Figure 5** (TiO_2-2O), the PDOS peak of O2p in **Figure 5f** at –4.738eV and –3.851eV is significantly lower than that at –4.358eV in **Figure 5** (TiO_2-2O), and the width of the PDOS peak increases by 0.735eV, indicating that the activity of electrons around O3c increases at high-energy levels. On the right-hand side of the Fermi energy level,

the resonance peaks of the Ti3d orbital and O2p orbital at 0.212eV decrease, and the width of the Ti3d orbital increases by 0.114eV, indicating that the difficulty of electron transition to the anti-bonding orbitals decreases. The formation of Ti5c-Cl bonds weakens the strength of the Ti5c-O3c bonds. In **Figure 5g**, there are obvious resonance peaks of the Ti3d and O3p orbital at -4.474eV. The PDOS peaks of the O3p orbital at –4.474eV and –3.926eV are significantly lower than that at –4.358eV in the figure (TiO_2-2O), and the width of the PDOS peak increases by 0.546eV, indicating that the electron localization of O3c at the low-energy level decreases. This suggests that the bonding interaction between Ti5c and O3c decreases, which is beneficial to the formation of the Ti5c-Cl bond.

4 CONCLUSIONS

The first-principles ab-initio calculations were used to investigate the adsorption mechanism of Cl_2 on a stoichiometric rutile TiO_2 (110) surface and surfaces with different bridge-oxygen defects, and the results are as follows:

(1) During the adsorption of Cl_2 on the stoichiometric surface of TiO_2 (110), all Ti6c(m) are the electron providers and O3c are the electron receivers. The chemical bond of the Cl_2 molecule does not break and Cl_2 enters the vacuum layer after the adsorption, indicating that there is no significant interaction between Cl_2 and the stoichiometric surface of TiO_2 (110).

(2) All the adsorption processes of Cl_2 on the surface of TiO_2 (110) with bridge-oxygen defects are chemical adsorption. During the adsorption of Cl_2 on the surface of TiO_2 (110) with one bridge-oxygen defect, there is electron enrichment between the Cl atoms and Ti6c, and Ti6c-Cl bonds are formed. During the adsorption of Cl_2 on the surface of TiO_2 (110) with one row of bridge-oxygen defects, there is electron enrichment between the Cl atoms and Ti5c, and Ti5c-Cl bonds are formed. The Mulliken overlap populations of the Ti5c-Cl bonds are larger than those of the Ti6c-Cl bonds, and the covalent-bonding interaction of the Ti5c-Cl bonds is stronger.

(3) By analyzing the behavior mechanism and relative-strength trend of the Cl_2 adsorbed on the surfaces of different defects, it can be seen that the bridge-oxygen defects on the surface of TiO_2 (110) can promote Cl_2 dissociation and increase the bonding probability between the Cl atoms and Ti atoms. With an increase of defects, the saturation of Ti decreases. The higher the number of the Ti-Cl bonds formed, the more stable are the adsorption structures and the more favorable are the formations of the Ti6c-Cl bonds and Ti5c-Cl bonds.

(4) During the adsorption of Cl_2 on the surface of TiO_2(110) with bridge-oxygen defects, the stability of the Ti6c-O3c bonds and Ti5c-O3c bonds on the surface decreases, and more electrons are transferred around the Ti6c-Cl bonds and Ti5c-Cl bonds, which is conducive to the formation of the Ti6c-Cl bonds and Ti5c-Cl bonds.

Acknowledgment

This work is supported by the National Natural Science Foundation Project of China (51674052, 51974046). The authors are grateful to the Chongqing Research Program of Basic Research and Frontier Technology (cstc2018jcyjAX0003).

5 REFERENCES

[1] F. S. Liu, G. Xie, Z. L. Yu, Y. Cui, L. Tian, Z. F. Nie, Y. D. Li, Research and development of titania powders by chlorination technology, Mater. Rev., 28 (**2014**), 113–118

[2] X. H. Liu, Y. G. Sun, Status quo and development of TiO_2 production in China, China Nonferrous Metall., 3 (**2018**), 43–52

[3] Y. P. Ma, H. X. Liu, B. L. He, B. Zhao, Research on Production Technology of Titanium Dioxide by Chlorination, Yunnan Chem. Technol., 46 (**2019**), 94–98

[4] H. Zhong, D. Q. Er, L.Y. Wen, Theoretical study on influence of CaO and MgO on the reduction of FeO by CO, Appl. Surf. Sci., 399 (**2017**), 630–637

[5] H. Zhong, L. Y. Wen, J. L. Li, J. Xu, M. L. Hu, Z. Q. Yang, The adsorption behaviors of CO and H_2 on FeO surface: A density functional theory study, Powder Technol., 303 (**2016**), 100–108, doi:10.1016/j.powtec.2016.09.017

[6] X. Y. Wu, A. Selloni, S. K. Nayak, First principles study of CO oxidation on TiO2 (110): the role of surface oxygen vacancies, J. Chem. Phys., 120 (**2004**), 4512–4516, doi:10.1063/1.1636725

[7] Z. X. Yang, R. Q Wu, G. D. Goodman, First-principles study of the adsorption of CO on TiO_2(110), Phys. Rev. B, 63 (**2001**), 15007, doi:10.1103/PhysRevB.63.045419

[8] D. C. Sorescu, J. T. Yates, First Principles Calculations of the Adsorption Properties of CO and NO on the Defective TiO_2 (110) Surface, J. Phys. Chem. B., 106 (**2002**), 6184–6199, doi:10.1021/jp0143140

[9] X. F Liu, X. Chang, L. Zhu, X. F. Li, High-efficiency helium separation through g-C_2O membrane: A theoretical study, Comp. Mater. Sci., 157 (**2019**), 1–5, doi:10.1016/j.commatsci.2018.10.022

[10] Y. T Wang, E. J. Zhao, J. D. Zhao, L. Fu, C. Ying, L. Lin, Prediction of novel ground state and high pressure phases for W_2N_3: First-principles, Comp. Mater. Sci., 156 (**2019**), 215–223, doi:10.1016/j.commatsci.2018.09.054

[11] O. R. Inderwildi, M. Kraft, Adsorption, diffusion and desorption of chlorine on and from rutile TiO_2 (110): A theoretical investigation, ChemPhyschem., 8 (**2007**), 444–451, doi:10.1002/cphc.200600653

[12] J. N. O'Shea, J. B. Taylor, L. C. Mayor, J. C. Swarbrick, J. Schnadt, Molecular damage in bi-isonicotinic acid adsorbed on rutile TiO_2 (110), Surf. Sci., 602 (**2008**), 1693–1698, doi:10.1016/j.susc.2008.03.005

[13] H. Perron, C. Domain, J. Roques, R. Drot, E. Simoni, H. Catalette, Optimisation of accurate rutile TiO_2 (110), (100), (101) and (001) surface models from periodic DFT calculations, Theor. Chem. Acc., 117 (**2007**), 565–574, doi:10.1007/s00214-006-0189-y

[14] C. Xiang, J. X. Zhang, Y. Lu, D. Tian, C. Peng, Electronic and optical properties of the spinel oxides $Mg_xZn_{1-x}Al_2O_4$ by first-principles calculations, Mater. Tehnol., 51 (**2017**), 735–743, doi:10.17222/mit.2016.296

[15] Q. L. Liu, Z. Y. Zhao, DFT study on microstructures and electronic structures of Pt mono-/bi-doped anatase TiO_2 (101) surface, RSC Adv., 5 (**2015**), 17984–17992, doi:10.1039/c4ra12671h

[16] S. D. Sohn, S. H. Kim, S. K. Kwak, H. J. Shin, Defect-associated adsorption of monoethanolamine on TiO_2 (110): An alternative way to control the work function of oxide electrode, Appl. Surf. Sci., 467 (**2019**), 1213–1218, doi:10.1016/j.apsusc.2018.10.233

[17] M. D. Segall, P. J. Lindan, M. J. Probert, C. J. Pickard, P. J. Hasnip, S. J. Clark, M. C. Payne, First-principles simulation: ideas, illustrations and the CASTEP code, J. Phys. Condens. Matter, 14 (**2002**), 2717–2744, doi:10.1088/0953-8984/14/11/301

[18] W. Yun, G. S. Hwang, Adsorption of Au atoms on stoichiometric and reduced TiO_2 (110) rutile surfaces: A first principles study, Surf. Sci., 542 (**2003**), 72–80, doi:10.1016/S0039-6028(03)00925-7

[19] M. C. Payne, T. A. Arias, J. D. Joannopoulos, Iterative minimization techniques for ab initio total-energy calculations: molecular dynamics and conjugate gradients, Rev. Mod. Phys., 64 (**1992**), 1045–1097, doi:10.1103/RevModPhys.64.1045

[20] S. Q. Wei, F. Wang, M. Dan, K. Y. Zeng, Y. Zhou, The role of high oxygen vacancy concentration on modification of surface properties and H_2S adsorption on the rutile TiO_2 (110), Appl. Surf. Sci., 422 (**2017**), 990–996, doi:10.1016/j.apsusc.2017.06.040

[21] Y. Pan, W. M. Guan, Origin of enhanced corrosion resistance of Ag and Au doped anatase TiO_2, Int. J. Hydrogen Energy, 44 (**2019**), 10407–10414

[22] Y. Zhang, C. R. Zhang, W. Wang, J. J. Gong, H. S. Chen, Density functional theory study of α-cyanoacrylic acid adsorbed on rutile TiO_2(110) surface, Comput. Theor. Chem., 1095 (**2016**), 125–133, doi:10.1016/j.comptc.2016.09.024

[23] T. Q. Wu, D. Cao, X. Y. Wang, Z. W. Jiao, Z. T. Jiang, M. G. Chen, H. L. Luo, P. Zhu, Structure of CO_2 monolayer on KCl (100), Appl. Surf. Sci., 339 (**2015**), 1–8

[24] Y. W. Wu, Z. Ali, Q. Lu, J. Liu, M. X. Xu, L. Zhao, Y. P. Yang, Effect of WO_3 doping on the mechanism of mercury oxidation by HCl over V_2O_5/TiO_2 (001) surface: Periodic density functional theory study, Appl. Surf. Sci., 487 (**2019**), 369–378